Journal of Arid Environments 184 (2021) 104335

Contents lists available at ScienceDirect

Journal of Arid Environments

journal homepage: www.elsevier.com/locate/jaridenv

Understanding dust sources through remote sensing: Making a case for CubeSats

Matthew C. Baddock [a,*], Robert G. Bryant [b], Miguel Domínguez Acosta [c], Thomas E. Gill [d]

[a] Geography and Environment, Loughborough University, Loughborough, LE11 3TU, UK
[b] Geography, University of Sheffield, Sheffield, S10 2TN, UK
[c] Ingenieria Civil y Ambiental, Universidad Autonoma de Ciudad Juarez, 450 N. Avenida del Charro, Ciudad Juarez, Chihuahua, 32315, Mexico
[d] Geological Sciences, University of Texas at El Paso, 500 W. University Avenue, El Paso, TX, 79968, USA

ARTICLE INFO

Keywords:
Mineral aerosol
PlanetScope
MODIS
Chihuahuan desert
Dust emission
Playa

ABSTRACT

Dust sources have been revealed through remote sensing, first regionally by ~1° resolution sensors (TOMS), then at sub-basin scale by moderate-resolution sensors (MODIS). Sensors with higher spatial resolution until recently were poorly temporally-resolved, precluding their use for systematic investigations of sources. Now, "CubeSat" constellations with high-temporal-and-spatial-resolution sensors such as PlanetScope offer ~3 m resolution and daily (to sub-daily) temporal resolution. We illustrate the spatio-temporal dust plume observation capabilities of CubeSat data through a dust event case study, Bolson de los Muertos playa, Chihuahuan Desert, Mexico. For the event, PlanetScope showed numerous discrete point sources, revealing variability of surface erodibility and emission over ~8% of a focus area at time of capture. The unprecedented detail of PlanetScope imagery revealed plume development where outer-playa sands and fluvial-deltaic inputs contact lacustrine silts/clays, consistent with field-studies. PlanetScope's high fidelity improves spatial quantification and temporal constraint of source activity, and we assess the spatio-temporal capabilities of CubeSat in context with other dust observation remote sensing systems. Compared to previous satellite technologies, CubeSats bring better potential to link remote sensing to field observations of emission. This leap forward in the remote sensing of dust sources calls for the systematic analysis of CubeSat imagery in source areas.

1. Introduction

For a more comprehensive understanding of the mineral dust cycle, there is a recognised need for improved spatio-temporal constraint on the sources of dust emission and their dynamics (Zender et al., 2003; Bullard et al., 2011; Shao et al., 2011; Heinold et al., 2016). Many of the fundamental properties of dust that govern its potential environmental impacts (i.e., particle size, mineral and chemical composition) are influenced by the particular source area it is emitted from. Sources are thus the 'launch pads' of mineral dust, and represent the start of its atmospheric lifecycle. Field-based observation of dust emission at source, however, is not straightforward, given the often remote and harsh environments where sources occur, as well as the dynamic and complex spatio-temporal nature of emission processes (Thomas and Wiggs, 2008; Field et al., 2009; Bullard, 2010; Bryant, 2013; Webb et al., 2016).

1.1. Remote sensing of dust sources: a brief review

Remote sensing has long provided significant advances in understanding the spatial distribution and temporal variability exhibited by contemporary dust sources. Improvements in spatial fidelity of sensors have in particular provided an impetus for interpreting the dust cycle and the nature of dust sources. The first multi-annual, global remote sensing studies of atmospheric dust loading established the dominant large-scale source regions, revealing the importance of closed hydrological basins (Prospero et al., 2002; Washington et al., 2003). Such basins were either inundated during the Pleistocene and/or undergo ephemeral flooding in modern climates, storing accumulated fines, the deflation of which makes them major sources (high frequency and/or high magnitude emission) of mineral dust. The Total Ozone Mapping Spectrometer (TOMS) provided landmark characterisation of dust sources in the early 2000s at a spatial resolution of ~1° ° (Prospero et al., 2002; Washington et al., 2003). Subsequent time-series observations of

* Corresponding author.
E-mail address: m.c.baddock@lboro.ac.uk (M.C. Baddock).

https://doi.org/10.1016/j.jaridenv.2020.104335
Received 26 June 2020; Received in revised form 29 September 2020; Accepted 30 September 2020
Available online 5 October 2020

dust at this scale revealed the intermittency and interannual variability of emission from key source regions, especially those outside of the principal Saharan Dust Belt (Mahowald et al., 2003, 2010; Zender et al., 2003; Bryant et al., 2007). Following the identification of major dust-emitting basins, ensuing remote sensing investigations of source regions focused on finer spatial scales, notably adopting a sub-basin scale of enquiry. This "drilling down" was motivated by knowledge that while individual, often huge, basins were identifiable as single large-scale entities, the actual locations of dust emission occurred at much smaller spatial scales within them, preferentially linked to certain geomorphology and surface types (Bullard et al., 2008, 2011).

Sub-basin focused studies were driven by improvements in sensor technology, especially the early-2000s advent of the daily (later twice daily) 0.25–1 km resolution hyperspectral Moderate Resolution Imaging Spectroradiometer (MODIS) (Muhs et al., 2014). The spatial scale offered by MODIS allowed remote sensing studies to pick out the individual contributions, dynamics and chronologies of dust emission from the mosaic of geomorphic settings and surface types within large basins. MODIS′ resolution proved highly appropriate for producing inventories of dust point sources within larger dust source regions (e.g. Bullard et al., 2008; Zhang et al., 2008; Lee et al., 2009, 2012; Walker et al., 2009; Baddock et al., 2011; Vickery et al., 2013; Hahnenberger and Nicoll, 2014; Kandakji et al., 2020). The hyperspectral capacity of MODIS additionally allowed the development of a range of image processing algorithms (e.g. Ackerman, 1997; Miller, 2003; Murray et al., 2016; Yue et al., 2017) and derived data products (e.g. 'Deep Blue Aerosol Optical Depth' (Hsu et al., 2013) and 'Dust Optical Depth' (Ginoux et al., 2010)). These approaches have enhanced detection and quantification of suspended dust via its optical and physical properties, and proved useful in the determination of emitting surfaces (e.g. Baddock et al., 2015; Yue et al., 2017).

MODIS′ spatial resolution in particular has contributed to quantifying and refining of the idea that dust emission is spatially-localized, displaying a 'hotspot' nature, from preferential source areas within a broader landscape (Gillette, 1999). Remote sensing at the sub-basin scale has revealed long term connections between hydrology and geomorphology (both controlling sediment supply and availability), and allowed quantification of different surfaces' potential for dust emission (Kocurek and Lancaster, 1999; Bullard et al., 2011). A frequent goal of the sub-basin, MODIS-led studies has been to understand spatial variations in dust emissivity to better represent surfaces in models, toward improved estimates of predicted emission (Zender et al., 2003; Bullard et al., 2011; Parajuli et al., 2014; Baddock et al., 2016; Parajuli and Zender, 2017).

1.2. New opportunities for observing dust emission at the sub-basin scale

The scale at which MODIS provides insights for characterising preferential dust sources is exemplified in Fig. 1. The Chihuahuan Desert of North America was broadly identified as a dust source region by TOMS-based global surveys (Prospero et al., 2002), and subsequently, moderate resolution data (AVHRR, Advanced Very High Resolution Radiometer, Rivera Rivera et al., 2010; MODIS, Baddock et al., 2011, 2016) were applied to elucidate the patterns of dust emission at a sub-basin scale. For instance, in the northern Chihuahuan Desert, both the long term distribution of dust-related satellite data products (processed to 10 km resolution) (Fig. 1a) and multi-annual dust event plume analysis (Fig. 1b and c) from MODIS have characterised the linkages between dust emission and surface geomorphology in the region. These approaches have highlighted the significance of ephemeral lake and low-relief alluvial systems as preferential sources.

Despite insights provided by moderate resolution sensors, the scale of these data means that processes driving dust uplift, operating as surface-boundary layer interactions, can only be inferred (Webb and Strong, 2011). At the level of detail provided by moderate resolution imagers, the heterogeneity in remotely sensed dust observations is largely a product of sensor spatial resolution. It therefore remains difficult to reconcile this resolution with field-based *in situ* investigations of emission which have revealed sub-MODIS-scale variations between eroding and non-eroding surfaces (Lee et al., 2009; Bryant, 2013; Sweeney et al., 2011; von Holdt et al., 2019; Cui et al., 2019).

In Earth observation for environmental monitoring, fundamental trade-offs exist between spatial and temporal resolutions in the repeat viewing of fixed locations (Cooley et al., 2017). Single platforms with sensors that achieve relatively high resolution surface imaging are usually associated with longer intervals between repeat coverage, such that their sampling prevents frequent observation of dust source activity (e.g. Landsat 8 at 0.03 km offering 16 day repeat in sub-tropical regions). Sensor technologies with off-nadir capabilities such as Satellite Pour l'Observation de la Terre (SPOT; revisit of 1–3 days in this mode) are often utilised for faster emergency response (e.g. Lui and Hodgson, 2016), but are not currently widely available nor archived with global coverage (d'Angelo et al., 2016). The critical importance of temporal sampling explains why daily-to-sub-daily observations from MODIS, and the even higher frequency data capture of the Spinning Enhanced Visible and Infrared instrument (SEVIRI) onboard the geostationary Meteosat Second Generation platform, have proved especially valuable in recording variations in global (Ginoux et al., 2012) and regional dust activity (Schepanski et al., 2007, 2009; 2012; Walker et al., 2009; Ashpole and Washington, 2013; Murray et al., 2016; Hennen et al., 2019), across moderate/coarse ground resolutions (0.25–10 km). New geostationary satellite platforms such as Himawari and GOES-R (~10 min sample time) have significantly improved dust source detection in regions beyond the Sahara (She et al., 2018; Kondragunta et al., 2018). However, the coarse spatial resolution (~2 km) of these sensors is insufficient for pinpointing local sources and detailed observation of dust emission processes (Sowden et al., 2018). Clearly, spatial resolution remains a key constraint for remotely observing, characterising and quantifying dust source behaviour.

Where Landsat is a single platform, and MODIS monitors from two satellite platforms (Terra and Aqua, with VIIRS (Visible Infrared Imaging Radiometer Suite) as a comparable afternoon follow-on), recent developments have led to development of miniaturised, multi-platform satellite constellations (e.g. da Silva Curiel et al., 2005) now often referred to as "CubeSats" or "NanoSats". With these constellations, extremely high spatial resolution (0.003–0.005 km) Earth observation is now achievable on a daily or better basis, through coverage achieved by the large number of platforms (Plekhov and Levine, 2018). CubeSat and NanoSat deployment has moved rapidly in Earth observation over the last five years (e.g. Villela et al., 2018; Crusan and Galica, 2019) and Planet Lab's suite of Dove satellites equipped with the PlanetScope sensor is one such novel constellation. Systematic interrogation of its finely-resolved spatial data now can provide insights into dust sources at very high resolution (0.002–0.005 km). Given the number of satellites in the PlanetScope constellation, depending on orbits, multiple images can be available for the same location for a given day, providing potential sub-daily, optimally sub-hourly, imaging capability (Plekhov and Levine, 2018). The short (<24 h) turnover between PlanetScope data capture and availability for download and processing is an added benefit for dust monitoring, analogous to the near real-time availability of MODIS data.

At time of submission, >100 3U CubeSat/Dove platforms (assigned via constellation Flocks; Kopacz et al., 2020) were in orbit, each mounted with the PlanetScope instrument (Planet Labs, 2020), imaging in four bands (Red, Green, Blue, Near-Infrared) with an orthorectified spatial resolution of ~3 m. Regular data from these satellites became available in early 2017, and with its frequent delivery of very high spatial resolution imagery, PlanetScope has been applied in a range of dynamic surface change studies (e.g. Cooley et al., 2017; Wikacsono and Lazuardi, 2018: Park et al., 2019). Given the progress achieved through improved sensor resolution, application of PlanetScope to observing dust sources represents a next step in remote sensing of mineral dust

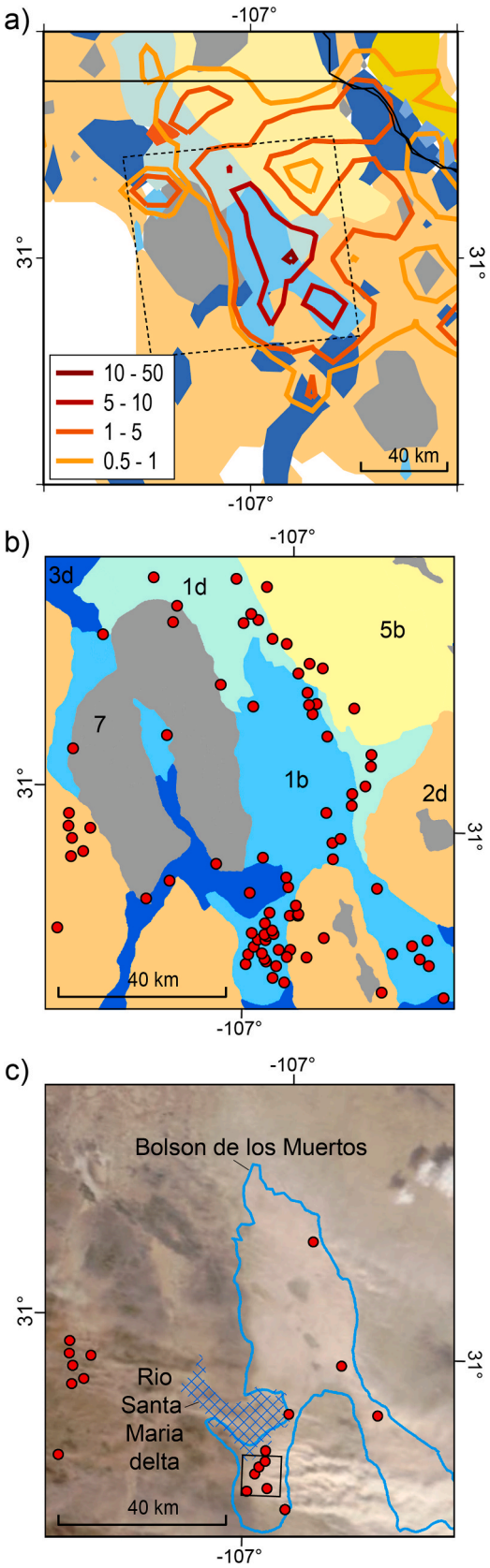

Fig. 1. Assessments of dust source activity in the northern Chihuahuan Desert, based on different moderate resolution MODIS data. a) Contours showing long term (2003–2014) dust loading as represented by Frequency of Occurrence (FoO % days) for MODIS Dust Optical Depth >0.75 (after Baddock et al., 2016), superimposed on the preferential dust source (PDS) geomorphological classification of emission potential (Bullard et al., 2011). Dashed box indicates focus of panels (b) and (c). b) Inventory of dust plume origin points 2001–2009 for the study region, as derived from inspection of true-colour MODIS scenes (Baddock et al., 2011), superimposed on the same PDS geomorphological classification (1b – ephemeral lake, 1d – dry, non-consolidated lake, 2d – high relief (unarmoured, unincised) alluvial systems, 3d – low relief (unarmoured, unincised) alluvial systems, 5b – aeolian sand dunes, 7 low emission surfaces) c) Example true-colour MODIS dust scene of a regional emission event (November 27, 2005) with plume origins marked. The extent of the Bolson de los Muertos playa is shown, with the blue crosshatch indicating the Rio Santa Maria paleo-delta feeding into the playa. Dashed box indicates focus of Fig. 2(c and d) in the southwestern arm of the playa. (For interpretation of the references to colour in this figure legend, the reader is referred to the Web version of this article.)

(caption on next column)

emission.

An inherent trade-off in sensor miniaturisation and payload optimisation for systems like PlanetScope, however, concerns the wavelengths sampled, such that PlanetScope provides only four proprietary wavebands. This relatively narrow spectral resolution reduces the opportunities for optimising dust detection afforded by a wider sampled spectral range, and in this paper, simple true-colour scenes are inspected. Despite an absence of multispectral dust enhancement procedures, and issues of subjectivity or inaccuracy in point mapping (Baddock et al., 2009; Walker et al., 2009; Sinclair and LeGrand, 2019), identifying dust plume origin points with true-colour imagery is an established means of mapping actively emitting portions of surfaces (e.g. Eckardt and Kuring, 2005; Lee et al., 2009; Hahnenberger and Nicoll, 2014; O'Loingsigh et al., 2015; Li et al., 2018; Nicoll et al., 2020). PlanetScope data are clearly well-suited for this purpose.

1.3. The potential of CubeSats for dust source identification: a case study

Herein we demonstrate the potential for understanding dust source characteristics that comes from enhanced satellite spatial resolution, specifically that provided by PlanetScope. We then go on to consider the place of these new data for improved characterisation of dust source dynamics. Our demonstration is used to consider how the capabilities of CubeSats and sensors like PlanetScope occupy a valuable niche in terms of the temporal and spatial constraints limiting remote sensing systems currently applied to dust observation. In a proof-of-concept study, we illustrate the performance of PlanetScope during a dust event occurring in one of North America's most persistent dust sources, presenting this in the wider context of insights that moderate resolution remote sensing provides for source areas in the region. We demonstrate the fact that PlanetScope now offers a spatial fidelity that improves remote detection of dust emission, and can closely augment field-scale observations of dust.

2. Method

2.1. Study location

To demonstrate the potential of high resolution imagery, an example from the northern Chihuahuan Desert is employed. The atmospheric dust loading from the Chihuahuan Desert and the region's importance for aeolian processes in the Western Hemisphere emerged in global remote sensing dust studies (Prospero et al., 2002; Ginoux et al., 2012). Further regionally specific studies have helped elucidate the erosivity and erodibility-related controls governing the dust activity (e.g. Lee et al., 2009; Rivera et al., 2010; Floyd and Gill, 2011; Baddock et al., 2011, 2016; Klose et al., 2019) (Fig. 1).

We focus on the Paleolake Palomas (PLP) basin, an extensive Pleistocene pluvial lake system spanning the present-day boundaries of Chihuahua (Mexico) and New Mexico (USA), which covered ~7700 km^2 at maximum extent (Dominguez Acosta, 2009). The basin now exists as a series of interconnected ephemerally-inundated playas (Castiglia and Fawcett, 2006) which serve as dust emission hotspots (Dominguez Acosta, 2009; Rivera et al., 2010; Baddock et al., 2011, 2016). The largest and southernmost of these playas, Bolson de los Muertos (BdlM), extends approximately 90 km north-south and up to 25 km east-west at its widest point. The BdlM consists of a wide central "body" with two "arms" (lobes) extending to the southwest and southeast (Fig. 1c). Each lobe is associated with an inputting river system that no longer enters the BdlM under contemporary conditions but was connected during late Pleistocene wet periods (Rio Santa Maria entering the SW lobe and Rio del Carmen the SE lobe) (Dominguez Acosta, 2009). Historical fluvial inputs associated with the discharge of the Rio Santa Maria into the SW lobe led to the deposition of deltaic sediments in portions of the playa (marked on Fig. 1c).

While lacking regular fluvial inflow in the present climate, the two individual lobes occasionally demonstrate "wet playa" behaviour (Rosen, 1994) associated with their status as regional topographical sinks. Acting as small endorheic basins, the lobes periodically accumulate water from major regional precipitation events, receiving in-washed alluvial sediment from surrounding higher elevations. This hydrological and sediment recharge behaviour modulates the lobes' activity as sources of dust, but contributes to the overall highly emissive nature of these playa surfaces in the longer term (Reynolds et al., 2007) (Fig. 1a and b).

For this case study, we consider the southwestern arm of the BdlM (SW BdlM), elongating approximately 30 km in a NNE direction and 9 km wide. The inner part of the SW BdlM is generally unvegetated, flat, devoid of non-erodible elements, and filled with fine (silty clay) clastic sediments, covered after evaporation of late summer monsoon moisture by a thin clay crust. Surrounding this inner core of playa sediments is a sparsely-vegetated (a few patches of grasses) marginal sand sheet augmented with fluvial-deltaic sediments to the northwest, deposited by the paleo-inflows of the Rio Santa Maria, and Quaternary alluvial deposits on the west, shed from the Cerros la Nopalera. These fluvial and alluvial sediments accumulated on the western and northern SW BdlM playa surfaces as graded beds ranging from clay and silts to small amounts of sand-sized sediments and some deltaic rounded gravels (Dominguez Acosta, 2009). Land use is very sparse and primarily livestock grazing, although irrigated cropland agriculture is practiced in isolated areas adjoining the BdlM and more widely in the floodplain of the modern Rio Santa Maria upstream. There is minimal land use of the playa surface itself.

The combination of strong westerly/southwesterly winds (perpendicular to the orientation of the PLP basin) during the dry season, and sands on the upwind outer margin of the playa that saltate onto the fine sediments in the playa's centre, leads to frequent emission of dust plumes from the BdlM. Such events are regularly identifiable on MODIS imagery (Lee et al., 2009; Rivera et al., 2010; Baddock et al., 2011) (Fig. 1b and c). Dust plumes from the BdlM, other sub-basins of PLP, and other sources regularly merge into regional-scale dust events which cause air quality hazards to the Ciudad Juarez (Chihuahua)-El Paso (Texas) metropolitan area (Rivera et al., 2010; Rivas et al., 2019) and can extend at least 800 km downwind across Texas (Lee et al., 2009).

Previous research has examined Chihuahuan Desert dust sources at a sub-basin scale, using the Preferential Dust Source (PDS) classification scheme (Baddock et al., 2011; Bullard et al., 2011). PDS was designed to represent observations that dust-yielding basins are comprised of different geomorphology or surface types, each with varying potentials to emit dust. The PDS surface classification effort was intended to understand the influence of variations in surfaces and their sediments on dust activity at a sub-basin scale (Bullard et al., 2011). The PDS scheme was applied to the Chihuahuan Desert (e.g. Fig. 1b), and is explained, by Baddock et al. (2011), who mapped attribution of PDS geomorphological classes to polygons of the Mexican national land type mapping system ("Sistema de Topoformas") as distributed by the national geospatial agency (INEGI, 2001). For the smaller scale of the current SW BdlM study, it was possible to use the more detailed national soil map polygons provided by INEGI (2001).

To help formalise the analysis of the dust event, a regular grid of 100 m^2 cells was generated over the polygon from the PDS scheme representing the entire BdlM (Fig. 1c). While application of this 100 m scale grid is somewhat arbitrary, in their review of wind erosion modelling, Webb and Strong (2011) propose the scale between what they term 'plot' (10^1) and 'landscape' (10^3) as the appropriate scale at which to consider emission processes. Analysing these 100 m cells is an appropriate scale to map emission detectable in (~3 m resolution) PlanetScope imagery.

2.2. Study dust event and satellite imagery

To illustrate a dust event detected via high resolution PlanetScope in the context of moderately resolved MODIS data for the region (Fig. 1), dust emission occurring at the SW BdlM was chosen from November 30, 2018. On this day, a strong Pacific cold front, aligned with an upper-level trough and extending southwestward from a cyclone centred in northeast New Mexico, crossed the northern Chihuahuan Desert from west to east. This produces an ideal synoptic weather pattern for dust storms in the region (Rivera et al., 2009). Winds gusted to 90 km/h at El Paso International Airport, ~140 km north-northeast of the SW BdlM; hourly PM_{10} concentration recorded by the Texas Commission on Environmental Quality at Socorro (southeast of El Paso and ~130 km northeast of the SW BdlM) reached 961 $\mu g/m^3$ while hourly $PM_{2.5}$ concentration reached 62 $\mu g/m^3$, both at 0900 MST (1600 UTC).

Imagery for the event was obtained from the Planet Labs exploration portal (www.planet.com) and the NASA Worldview site for pre-processed MODIS data. We examine true-colour imagery of SW BdlM from PlanetScope (1706 UTC capture time), and MODIS Terra (1735 UTC) and Aqua (2050 UTC). For PlanetScope, bands 1–3 (Blue: 455–515 nm, Green: 500–590, Red: 590–670 nm) of the Level 3B Analytic Ortho Scene Product in GeoTIFF format were obtained and composited to produce simple true-colour scenes. Two scenes from 1706 UTC imaged along the same sensor overpass (37 and 38 s past the minute) were used in a mosaic over the SW BdlM study area.

3. Results

A broad view of the November 30, 2018 BdlM dust event is shown by the Terra and Aqua MODIS scenes (Fig. 2a and b). MODIS imagery quality for the event is relatively poor, due to inherent problems of native resolution (WorldView imagery resampled to 250 m) and pixel stretch near the edge of the image swath, but the MODIS true-colour data reveal dust in a part of the playa known to emit often. In the Aqua scene, an elevated plume is most clearly visible heading eastward, showing a typical dust uplift pattern with the passage of a Pacific cold front (cf. Fig. 1c). A best-estimate of the upwind point of the plumes identifies active emission in the SW BdlM, which the long term point source inventory indicates is an area prone to emission (Fig. 1b).

PlanetScope overpasses covering the event were available from ~30 min before the Terra overpass. Analysis of the PlanetScope data reveals numerous discrete, identifiable dust plumes in the SW BdlM, whose upwind extent can be tracked to specific emitting parts of the playa surface (Fig. 2c [A high resolution image of this figure panel is available in the Supplementary Material]). Directly comparing the best interpretation of the true-colour MODIS and PlanetScope scenes, the MODIS points coincide fairly well with the most well-developed coalesced plumes shown on PlanetScope, <2 km of their apparent upwind origins (Fig. 2d). Crucially however, many more smaller plumes are identifiable via PlanetScope from multiple parts of the playa, providing much more

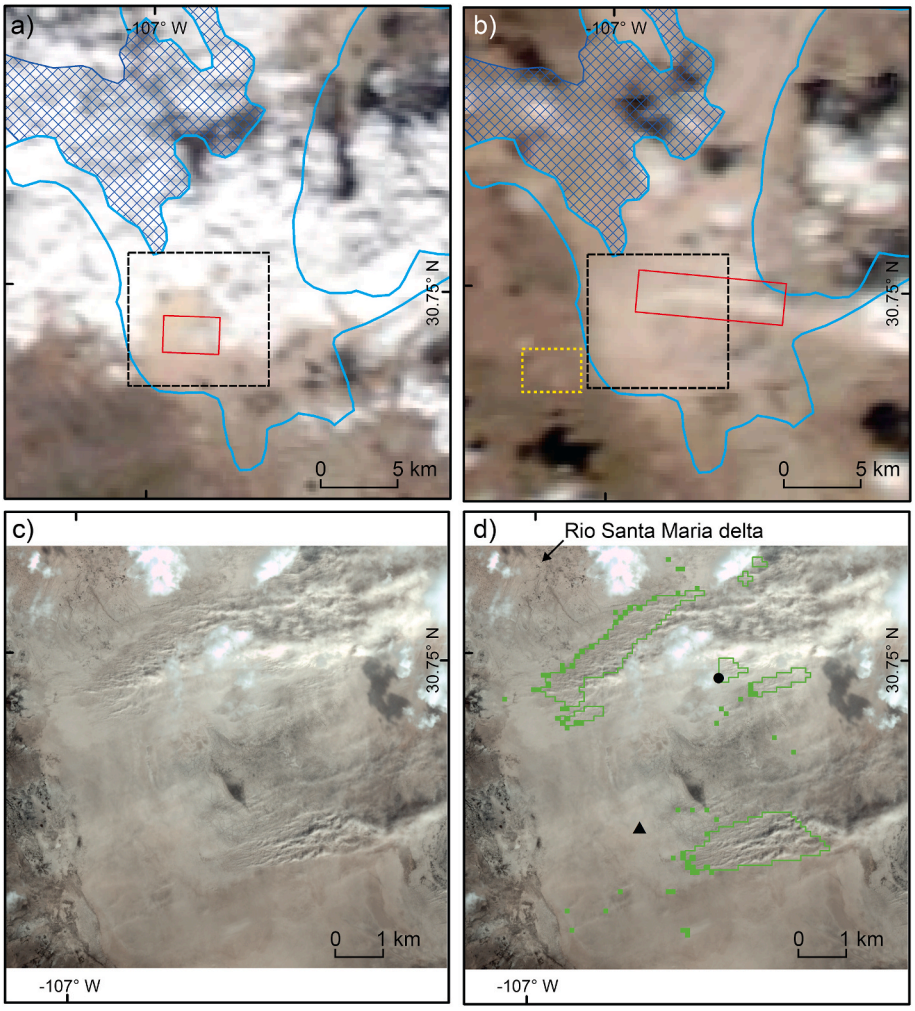

Fig. 2. a) Terra MODIS (1735 UTC) true-colour scene of November 30, 2018 dust event showing the faint presence of dust visible on the south-western lobe of the of Bolson de los Muertos playa. Red box highlights the plume over the playa surface, before presence of cloud to the east obscures plume. Plume interpreted with a comparison to dust-free MODIS scene (not shown). Hashed lines show extent of the Rio Santa Maria paleo-delta from INEGI (2001) national soil map. Pixel resolution 250 m. Dashed black box shows focus of figure panels (c) and (d). b) Aqua MODIS (2050 UTC) from the same day showing presence of a more apparent dust plume slightly further to the north in the focus area. Red box highlights plume extending to the east. Dashed yellow box shows focus of Fig. 5 c) PlanetScope (1706 UTC) true colour scene of November 30, 2018 dust event, showing emission occurring in the south-western arm of Bolson de los Muertos playa. Pixel resolution 3 m. Note some cloud is present, but less than shown in MODIS at 1735 UTC. (A high resolution version of this panel is available in the Supplementary Material.) d) Grid cells where surface emission can be estimated from plumes identifiable in PlanetScope, for a regular 100 × 100 m grid over the southwest arm of the Bolson de los Muertos. Solid cells – cells containing discernible upwind initiation points of small plumes shown in (c). Open cells – cells with evidence of likely emission from the surface, shown by multiple individual small scale plumes, close to the surface, and located downwind of solid cells containing discernible initiation. Black triangle and circle indicate apparent plume source estimated from Terra and Aqua images (a, b) respectively. (For interpretation of the references to colour in this figure legend, the reader is referred to the Web version of this article.)

detail and accuracy concerning the specific parts of the surface that are emitting.

When applied to the regular 100 m^2 grid placed over the BdlM, those grid cells where emission and plume initiation could unambiguously be identified at the upwind edge of the lofted plumes are highlighted (Fig. 2d). The area of focus indicated in Fig. 2a and b represents an approximately 8.25 km square section (68.3 km^2). Image interpretation indicates that 68 cells contained the onset of plumes at the upwind boundaries of emission (Fig. 2d), equating to ~1% of the focus area. MODIS-based studies have identified a significant bias in favour of identification of upwind source points in point inventories (e.g. Lee et al., 2009, 2012; also SEVIRI, Hennen et al., 2019), due to the inability to detect discrete points invisible underneath the main plume. This limitation largely restricts determination of source points to those at the upwind "plume heads" (Walker et al., 2009; Sinclair and LeGrand, 2019). Whilst also an issue for interpretation of the PlanetScope imagery, the increased level of detail from PlanetScope offers increased ability to ascertain those surfaces that are actively emitting downwind from the upwind boundary of emission. In Fig. 2d, additional cells estimated as being highly likely to contain emission, as evidenced by the presence of multiple plumes appearing close to the surface, and downwind of discernible upwind initiation, are also indicated. These additional 499 cells account for a further ~7.3% of the area, indicating evidence of dust emission occurring in total over ~8% of the focus portion of SW BdlM.

4. Discussion

4.1. Pinpointing dust point source locations and geomorphology from high resolution imagery

Here, in showing PlanetScope imagery over a source area during a dust emission event, we demonstrate how its high resolution allows direct observation of active plume development to an unprecedented degree. That the imagery allows pinpointing of the upwind origin of individual dust plumes to precise emission surfaces and small-scale geomorphic setting emphasises the detail of emission processes that can be unlocked from these high resolution images. This capability achieves insights into the spatial heterogeneity of processes and emission far beyond that revealed by moderate resolution sensing (Fig. 1; Fig. 2).

For instance, PlanetScope reveals that the cluster of dust plumes initiating from the outer northwest portion of the BdlM focus area (Fig. 2c and d) is located in a zone where numerous small washes terminate, indicating where sediments of mixed sizes from the Rio Santa Maria paleodelta are likely to have been brought onto the playa. This line of washes and presence of fluvial material extends to the northeast, with the distribution of active dust emission grid cells also stretched in that direction. This location is also consistent with areas where playa-marginal sands, undergoing saltation by W-WSW wind, would move onto lacustrine clays dominating the inner playa surface. Such contact zones in playa basins are well known to become preferential dust sources due to the combination of loose sands for saltation bombardment over

fine sediments (Cahill et al., 1996; Gill, 1996; Lee et al., 2009; Rivera et al., 2010; Bullard et al., 2011).

The multiple dust plumes in the central part of the playa shown by PlanetScope, close to the source point evident from Aqua MODIS, also reveal emission occurring further from the edges and availability of aeolian or fluvial inputs, which potentially reflects the action of other emission drivers (Fig. 2d). Dust emission here may be associated with areas of weakly-crusted playa surface, susceptible to breakage and auto-erosion, exposing unconsolidated silt-clay sediments underneath to the wind, as documented on other parts of the BdlM (Dominguez Acosta, 2009) and at Owens Lake (Cahill et al., 1996). The most southerly cluster of dust plumes revealed by PlanetScope in the scene is again consistent with W-WSW winds entraining sand sheet sediments from the upwind outer playa, bringing them into contact with finer lacustrine clays and silts, to drive dust emission. In addition, the long fetch in the direction of wind run across the flat playa likely contributes to a high potential for emission from erodible surfaces downwind (Cahill et al., 1996; Gillette, 1999). Clearly, the detail in which aeolian processes can be interpreted from PlanetScope is much improved over the equivalent MODIS data. Although Fig. 2d indicates broad spatial agreement between the MODIS-estimated plume origins and the pinpoint distribution from PlanetScope, an enhanced ability to interpret processes stems from improved accuracy in determination of emission points in high resolution data (Sinclair and LeGrand, 2019). In source identification studies led by moderate resolution sensors with daily sampling rate, uncertainty can exist whether the upwind edge of a plume is associated with active emission at the time of capture (Schepanski et al., 2007, 2009). Here, when PlanetScope overpass clearly occurs some time after the onset of emission, the detail of scene resolution allows plumes to be unambiguously traced back to ongoing, active emission (Fig. 2c).

A comparable dust-free scene of the SW BdlM from a few days before the study event, is valuable for characterising contemporary surface state, and its temporal change, in a system such as a playa (Fig. 3) (Reynolds et al., 2007; Urban et al., 2018). For instance, PlanetScope detail in the dust-free image is sufficient to identify large polygon-shaped desiccation peds (characteristic of the BdlM in general (Dominguez Acosta, 2009)), indicating the high clay and silt concentrations, and surfaces previously inundated by water. Fig. 3 also specifically indicates dust was not emitted from the central portion of the focus area, where the surface appears visibly darker. This darker surface indicates the presence of vegetation at the time, as evidenced by comparison of vegetated channels and arroyos seen off the playa, most notably to the west. Where vegetation likely to be of remnant state acts as non-erodible cover on the central portion of the playa saltation bombardment will be impeded (Lancaster and Baas, 1998), thus limiting plume development. Inspection of the dust-free imagery helps to account for this control on emission.

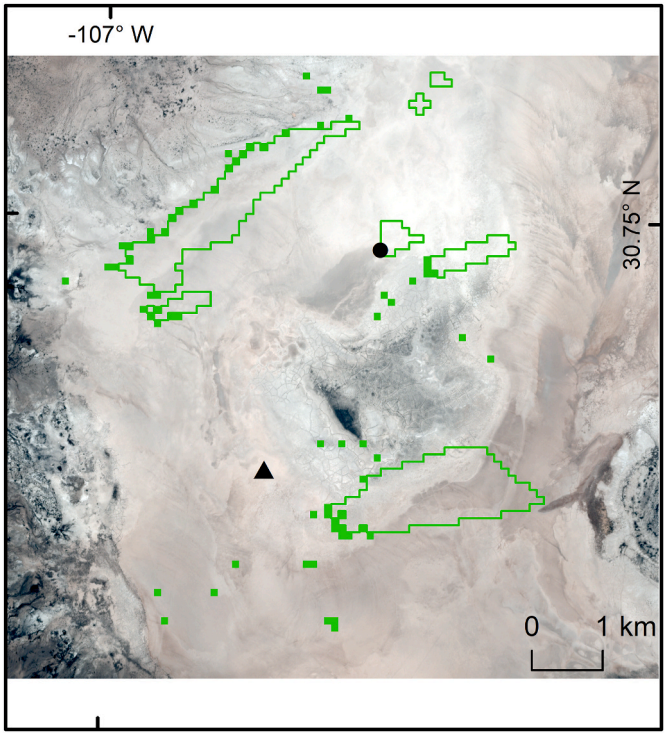

Fig. 3. True colour PlanetScope scene (November 27, 2018, 1722 UTC) depicting focus section of the southwest arm of the Bolson de los Muertos playa surface three days before the dust event in Fig. 2. Solid squares are the upwind emitting grid cells, open green polygons are the broader downwind estimates of emitting surface from Fig. 2d. (For interpretation of the references to colour in this figure legend, the reader is referred to the Web version of this article.)

In summary, the detail provided by the PlanetScope imaging of plume sources reinforces the broader importance for dust emission of contacts between different geomorphic domains. In this case, the known connectivity between saltator availability at playa margins, fluvially-provided wind-suspendible fines, and lacustrine sediment of variably crusted state is emphasised for the first time in satellite imagery. These and other linkages can be determined by interpretating the locations where emission points can be unambiguously pinpointed (Mahowald et al., 2003; Lee et al., 2009; Bullard et al., 2011; Klose et al., 2019).

4.2. Scale limits for dust source monitoring using PlanetScope data

In order to understand dust emission processes, one of the key challenges has been to match remote sensing observations to the space and time scales of field-observed emission (Bullard, 2010; Bryant, 2013). The BdlM dust source observations in our case study enable reflection on the relative contribution of remote sensing data to both dust source and dust plume detection, and how these relate to improved understanding of emission. The relative scales at which commonly used remote sensing data are able to characterise dust emission events are summarised in Fig. 4. When considering these, a number of studies acknowledge the small scale and stochastic nature of the dust emission process (e.g. Gillette, 1999; Lee et al., 2009; Bullard et al., 2011; Shao et al., 2011; Kok et al., 2014*et a*). Field and modelling studies in and around playa basins (e.g. Cahill et al., 1996; King et al., 2011; Sweeney et al., 2011; von Holdt et al., 2019) have highlighted the variability of surface erodibility and the importance of crusts for the dust emission process. Haustein et al. (2015) go one step further, matching the scale of emission to dust modelling schemes, highlighting how surface heterogeneity can lead to significant uncertainty in model estimates. Using the most informative studies in terms of the spatial scale of emissions, such as Webb and Strong (2011) and Haustein et al. (2015) as a baseline, we infer an approximate "scale limit" (c. 10^2 m and <1 day) for dust source detection that is able to capture site information appropriate to the scale of surface erodibility heterogeneity. This is the scale that can be complementary to *in situ* observation of emission. For understanding the contribution of remote sensing, this "scale limit" therefore represents an arbitrary divider between remote sensing detection of dust emissions observed at the field-scale (thereby linked to process), and dust plumes evident at the basin and sub-basin scale (from which we must infer process). Temporally, it is clear that observations captured sub-daily are also essential to establish the locations of dust emission (Schepanski et al., 2009; Shao et al., 2011; Webb et al., 2019; Klose et al., 2019); such observations are possible with the PlanetScope data (Fig. 5).

Webb and Strong (2011) provide a robust framework for the spatial and temporal scales at which dust emission and transport operate. A summary of how these processes are sampled by remote sensing data types is provided in Fig. 4, and we use our emission scale limit to consider the likely detection of dust in transport, or, dust emission at source. In terms of temporal resolution, we note that the frequency of dust event detection (e.g. as observed from synoptic weather code

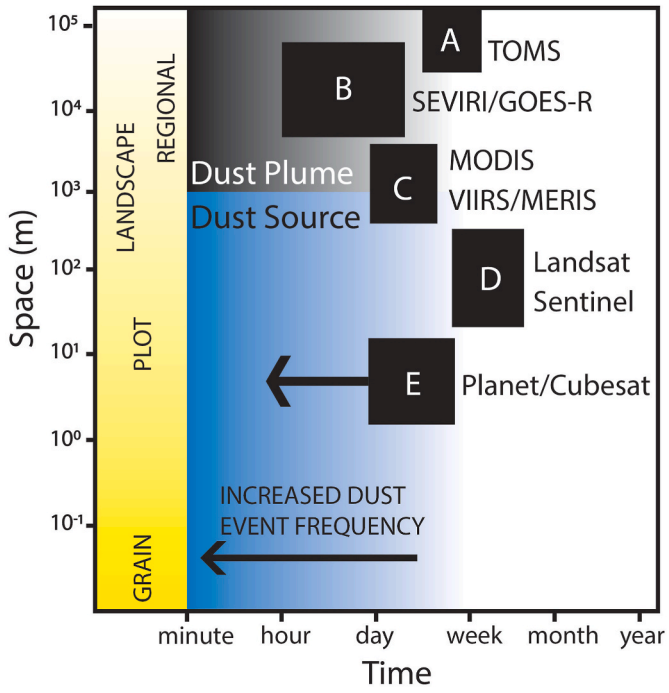

Fig. 4. Conceptual figure characterising time and spatial scales of dust emission and dust transport (i.e. plume passage) phenomena, in relation to the monitoring/detection capabilities of existing satellite systems, and the niche of CubeSats (e.g. PlanetScope), from this study. We use the spatial scale limits suggested by Strong and Webb and Strong (2011) to highlight that the spatial resolution, in which most remote sensing observations operate, obviates plot-scale of understanding dust emission processes. In the temporal, most studies are unable to sample at a scale where a representative sample of dust events will be captured, compared to field-based (e.g. Klose et al., 2019) or meteorological data-based (e.g. O'Loingsigh et al., 2010) approaches. Black boxes represent realistic limits in dust source/plume detection based upon published studies (A: TOMS, Bryant et al., 2007; B: SEVIRI, Murray et al., 2016; C: MODIS, Baddock et al., 2009; D: Landsat/Sentinel, von Holdt et al., 2017; Bakker et al., 2019, E: CubeSat/PlanetScope; this study.).

reports at WMO sites; O'Loingsigh et al., 2010) increases significantly at a sub-day frequency (e.g. Novlan et al. (2007) for the northern Chihuahuan Desert). Fig. 4 shows that most current dust remote sensing applications work outside the required lower scale limit. Initial source detection efforts using TOMS (e.g. Prospero et al., 2002, Fig. 4, A) were only able to identify candidate basin-scale dust sources and subsequently relate the dynamics of these to regional climate and landscape scale processes (e.g. Bryant et al., 2007). At a basin and sub-basin scale, geostationary satellites (e.g. SEVIRI: Schmetz et al., 2002; Himawari: Bessho et al., 2016) have been used to detect, track and characterise dust emissions over large regions (e.g. Schepanski et al., 2009; Banks and Brindley, 2013, Fig. 4, B). In practice, these data have been used to (i) detect and build inventories of dust events used to infer source regions (e.g. Hennen et al., 2019), (ii) match events to synchronous data to determine climatological drivers of emission over short (<day) to decadal timescales (e.g. Schepanski et al., 2009; Gasch et al., 2017), and (iii) provide quantitative estimates of dust properties and radiative impacts (e.g. Brindley et al., 2012). Where these data have been used to detect and identify dust events at the sub-basin scale (e.g. Murray et al., 2016; Hennen et al., 2019) they are often only able to track clearly visible plumes locations to within 3–8 km of likely source location, making links between plot-scale emission processes and dust events difficult to resolve (Fig. 4, B).

Data from moderate resolution sensors (e.g. MODIS, VIIRS; Fig. 4, C), have also been used extensively to observe plumes close to dust sources either involving subjective analyses (e.g. Bullard et al., 2008; Baddock et al., 2009; Lee et al., 2009, 2012) or the use of processed, dust-related data products (e.g. Ginoux et al., 2010, 2012; Baddock et al., 2016). The increased spatial resolution of MODIS-like data produces a shift towards the suggested scale limit, thereby enhancing characterisation of dust emission hot spots and their candidate geomorphic settings. Synergistic use of data from these moderate resolution sensors has also increased our understanding of dust sources and transport corridors (e.g. Bakker et al., 2019). As an Earth monitoring system, the combination of Sentinel 2A/B and Landsat 8 (Fig. 4, D) offers the ability to determine dust emission at a scale which may approach the required scale limit. The image resolution and image scene size of these data certainly facilitate dust plume interpretation at the sub-basin and landform scale (e.g. von Holdt et al., 2017, 2019), however, the best combined revisit period for these data for most areas (c. 5 days) still falls below that required to capture dust emission data sufficiently regularly to usefully match field observations (e.g. Li and Roy, 2017). In our case study, we show the relative advance that PlanetScope data, and CubeSat-constellation observation systems in general, can make through high spatial and temporal observation of dust source dynamics, operating *inside* the suggested space/time scale limits for plot-scale monitoring proposed here (Fig. 4, E).

4.3. *Benefits of dust emission monitoring via CubeSats*

The analysis provided in Fig. 2 indicates how future in-depth studies might characterise specific emission locations with greater space/time fidelity than can moderate resolution sensors, and thereby may better inform representation of surface types within dust emission models. Dust emission characterisation through PlanetScope's high resolution imagery is clearly relevant to the small scale parameterisations required to improve large-scale dust modelling (Thomas and Wiggs, 2008; Bullard, 2010). Within an area of land surface known to be highly emissive, in this example <10% of the surface was assessed to be unambiguously emitting at one time during the study dust event (Fig. 2d). At the scale of the PDS classification, the whole of BdlM is uniformly classified as "ephemeral playa" (class 1b; Bullard et al., 2011). PlanetScope, however, establishes the actual spatial variability of emission within this single MODIS-scale surface class, helping to account for variability in emission potential observable in the field (e.g. von Holdt et al., 2019; Klose et al., 2019; Cui et al., 2019).

Another key benefit of high resolution monitoring of aeolian processes is an improved ability to constrain timing of dust uplift and the role of small-scale meteorological processes in dust emission, approaching comparability with field-based observations (Fig. 5). The contribution of high temporal frequency remote sensing in this regard has been demonstrated for SEVIRI (e.g. Schepanski et al., 2009). Future studies that couple high spatial resolution imaging with high temporal resolution ground-based measurement of key meteorological variables (the latter primarily related to determining transport capacity i.e. shear velocity, turbulent gusting etc.), will combine "top down" and "bottom up" perspectives of dust emission (Richter and Gill, 2018) with better fidelity. Detailed ground observation studies such as the intensive remote camera-based dust monitoring of Soda Lake, a Mojave Desert playa, by Urban et al. (2018), are one way to evaluate the level of dust activity that PlanetScope can additionally retrieve.

Aside from the transport capacity-limitation (wind threshold exceedance), dust uplift in most global dust source areas is also limited by two other factors; (i) sediment availability, and/or (ii) sediment supply (Kocurek and Lancaster, 1999; Bullard et al., 2011). When considering the sediment availability-limitation, the temporary flooding of a surface, such as the BdlM playa, often followed by vegetation growth and/or development of surface crusting, leads to dust-sized sediment not being available to erode. After drying or crust weakening, this availability-limitation becomes relaxed, and sources may emit again (Mahowald et al., 2003; Bryant et al., 2007). Periodic 'switching off-switching on' of dust emission is a fundamental aspect of variability

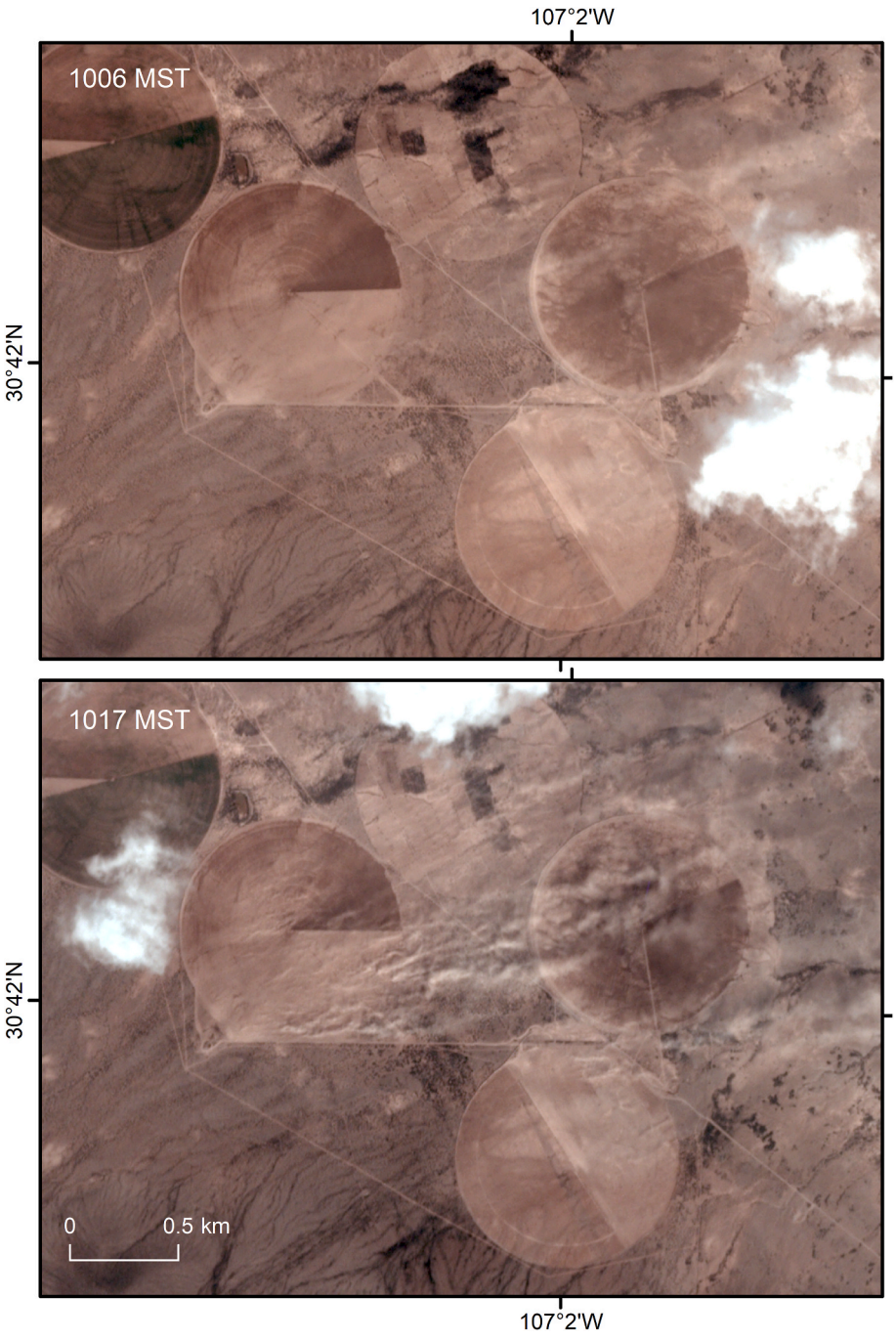

Fig. 5. PlanetScope overpasses available 11 min apart, achieved by the Planet CubeSat constellation for the November 30, 2018 regional dust event. The image sequence helps constrain the spatial occurrence and temporal onset of dust emission from centre-pivot irrigated field systems during the day's dust event. A 1003 MST (1703 UTC) overpass was also available for this site. Area of focus is shown by yellow box in Fig. 2b. (For interpretation of the references to colour in this figure legend, the reader is referred to the Web version of this article.)

in dust source activity, and must be accounted for in the accurate simulation of regional dust regimes. Detailed imagery such as from PlanetScope will enable daily monitoring of emissions from specific surfaces, revealing both when and where they begin to be emissive, and crucially, when and where they do *not*. While timing of overpasses will remain an issue for capture of emission, the repeat spatial resolution of CubeSats can nevertheless better establish controls on (i) geomorphic thresholds of emission, and (ii) temporal constraints on dust uplift. In the latter case, linkage of pinpoint emission observation to key meteorological parameters, including *in situ* measurements where possible (e.g. Haustein et al., 2015), and to hydrological histories of the location (inundation and drought regime), can help validate dust modelling efforts.

Finally, we suggest how the unprecedented detail of CubeSat data can guide enquiry into dust emission for both future remote sensing technologies and field observations. For instance, one important contribution will be the opportunity to help target remote sensing missions such as the Earth Surface Mineral Dust Source Investigation (EMIT; Thompson et al., 2020), by providing enhanced understanding of the dynamics of dust emission surfaces (especially crust distribution and types). In terms of field-based measurement of dust flux and/or emission potential of surfaces, von Holdt et al. (2017, 2019) demonstrated how the relatively high spatial resolution of Landsat data aided the location of field campaigns to test emissions from different surfaces. The increased space/time precision of source mapping offered by sensors like PlanetScope will be invaluable for guiding field studies designed to quantify dust emission rates from surface types within landscapes (King et al., 2011; Sweeney et al., 2011; Bryant, 2013; Klose et al., 2019). Additional to the long term (multi-annual) monitoring of emission surfaces, we note that the rapid delivery of PlanetScope data after

collection, and the near real-time provision of imagery, will permit observation of dust events almost as they unfold. Such a facility benefits field studies and other *in situ* observation campaigns such as fixed-point air quality monitoring, and for purposes of fugitive dust identification and wind erosion mitigation (e.g. Miller et al., 2012; Kandakji et al., 2020).

4.4. Some limitations of CubeSat data for dust source observation

In terms of their application to observing dust within source areas, some limitations of CubeSat and the PlanetScope data used here specifically, require noting. Considering the role of CubeSats for observing dynamic surface change phenomena, Cooley et al. (2017) emphasise that constellation-derived imagery is acquired by way of smaller, lower budget sensors such that radiometric quality, consistency and signal-to-noise ratios are below that of missions supported by major space agencies. The large number of individual platforms comprising any constellation unavoidably produces inconsistency about cross-sensor calibration, image quality and accuracy of geolocation, all of which represent general limitations. For PlanetScope geolocation error is reported <10 m (Planet Labs, 2020), but given the scale at which dust emission can be considered, any such inaccuracy was effectively mitigated within the 100 m grid source cell approach adopted here.

With the high albedo caused by often limited vegetation and typically light-coloured sediments in dust source areas, many sources are characterised by bright surfaces which can confound observation of plumes using only visible bands (Kaufman et al., 2002; Miller, 2003; Zhang et al., 2008). With only one non-visible band, opportunities for algorithmic enhancement of dust in PlanetScope data are limited. While recognising this issue, in this study we focused on interpretation of basic true-colour scenes, and as we demonstrate, problems of plume definition are mitigated to some extent by the excellent spatial resolution. CubeSat sensors may be especially prone to signal saturation over bright surfaces, precluding plume detection in the worst cases. This point, however, should be regarded next to the issue that dust detection over bright surfaces can be problematic even for multi-spectral sensors such as MODIS and SEVIRI (Baddock et al., 2009; Schepanski et al., 2009). 'Clear sky differencing', where dust-free images are subtracted to emphasise the presence of dust has proven a fruitful approach (Murray et al., 2016). The regular repeat viewing provided by CubeSats means that recent clean scenes required for background subtraction should be readily available (Fig. 3). This facilitates clear sky differencing as a straightforward way to potentially enhance the appearance of dust plumes from CubeSat imagery. The presence of cloud is a known complication for remote methods of dust detection (Ackerman, 1997; Miller, 2003; Baddock et al., 2009), and the absence of any inherent cloud masking processing for CubeSat data increases the need for user interpretation of scenes (Cooley et al., 2017).

5. Conclusion

Advances in the spatial and temporal resolution of terrestrial remote sensing over the past two decades have revealed the sources of aeolian dust with improving spatial and temporal fidelity. Our case study suffices to show that the extreme spatial detail, coupled with daily/sub-daily global coverage available from CubeSats such as PlanetScope, provides a leap forward in our ability to monitor aeolian dust dynamics through remote sensing. We offer a number of concluding remarks:

- We demonstrate the capabilities and potential benefits for understanding dust source behaviour achievable with highly-spatially-resolved imagery now readily available on a daily basis with global coverage.
- We show that the detail in which dust plumes can be captured with PlanetScope data now allows visualisation of dust emission at a scale which, for the first time, can realistically augment field measurements. The daily availability of data is comparable to moderate resolution sensors, but the opportunity for sub-daily constellation-based CubeSat imaging also provides considerable additional potential. Considering other remote sensing systems currently used for dust source observation, coupling CubeSat performance with hyper-temporal monitoring of dust source activity (e.g. via SEVIRI, GOES-16/17), will significantly enhance our ability to monitor and understand source dynamics.
- Taking advantage of its unprecedented detail and global coverage, we call for future, systematic evaluations of constellation-based, high spatial resolution imagery. These data provide a new impetus for informing our understanding of the spatio-temporal distribution of aeolian processes, the drivers of aeolian processes within the global dust cycle, and their representation in regional and global climate models.

CRediT authorship contribution statement

Matthew C. Baddock: Conceptualization, Methodology, Formal analysis, Writing - original draft. **Robert G. Bryant:** Conceptualization, Methodology, Writing - original draft. **Miguel Domínguez Acosta:** Writing - original draft, Writing - review & editing. **Thomas E. Gill:** Conceptualization, Methodology, Writing - original draft.

Declaration of competing interest

The authors declare that they have no known competing financial interests or personal relationships that could have appeared to influence the work reported in this paper.

Acknowledgments

The authors acknowledge Planet Labs for their provision of free data access to education and research users. Mark Szegner at Loughborough helped with cartography, and we are grateful for the detailed comments of two reviewers and Editorial input. This work was inspired by a Royal Geographical Society (with the Institute of British Geographers) Small Research Grant (SRG 15/17) to MCB, and NASA support (grant 80NSSC19K0195) to TEG.

Appendix A. Supplementary data

Supplementary data to this article can be found online at https://doi.org/10.1016/j.jaridenv.2020.104335.

References

Ackerman, S.A., 1997. Remote sensing aerosols using satellite infrared observations. J. Geophys. Res. 102, 17069–17079.
Ashpole, I., Washington, R., 2013. A new high-resolution central and western Saharan summertime dust source map from automated satellite dust plume tracking. J. Geophys. Res. 118, 6981–6995.
Baddock, M.C., Bullard, J.E., Bryant, R.G., 2009. Dust source identification using MODIS: a comparison of techniques applied to the Lake Eyre Basin, Australia. Remote Sens. Environ. 113, 1511–1528.
Baddock, M.C., Gill, T.E., Bullard, J.E., Dominguez Acosta, M., Rivera Rivera, N.I., 2011. Geomorphology of the Chihuahuan Desert based on potential dust emissions. J. Maps 7, 249–259.
Baddock, M.C., Parsons, K., Strong, C.L., Leys, J.F., McTainsh, G.H., 2015. Drivers of Australian dust: a case study of frontal winds and dust dynamics in the lower Lake Eyre Basin. Earth Surf. Process. Landforms 40, 982–1988.
Baddock, M.C., Ginoux, P., Bullard, J.E., Gill, T.E., 2016. Do MODIS-defined dust sources have a geomorphological signature? Geophys. Res. Lett. 43, 2606–2613.
Bakker, N.L., Drake, N.A., Bristow, C.S., 2019. Evaluating the relative importance of northern African mineral dust sources using remote sensing. Atmos. Chem. Phys. 19, 10525–10535.
Banks, J.R., Brindley, H.E., 2013. Evaluation of MSG-SEVIRI mineral dust retrieval products over North Africa and the Middle East. Remote Sens. Environ. 128, 58–73.
Bessho, K., Date, K., Hayashi, M., Ikeda, A., Imai, T., Inoue, H., Kumagai, Y., Miyakawa, T., Murata, H., Ohno, T., Okuyama, A., 2016. An introduction to Himawari-8/9—Japan's new-generation geostationary meteorological satellites. J. Meteorol. Soc. Jpn. Ser. II 94, 151–183.

Brindley, H., Knippertz, P., Ryder, C., Ashpole, I., 2013. A critical evaluation of the ability of the Spinning Enhanced Visible and Infrared Imager (SEVIRI) thermal infrared red-green-blue rendering to identify dust events. Theoretical analysis. J. Geophys. Res. 117, D07201.
Bryant, R.G., 2013. Recent advances in our understanding of dust source emission processes. Prog. Phys. Geogr. 37, 397–421.
Bryant, R.G., Bigg, G.R., Mahowald, N.M., Eckardt, F.D., Ross, S.G., 2007. Dust emission response to climate in southern Africa. J. Geophys. Res. 112, D09207.
Bullard, J., 2010. Bridging the gap between field data and global models: current strategies in aeolian research. Earth Surf. Process. Landforms 35, 496–499.
Bullard, J., Baddock, M., McTainsh, G., Leys, J., 2008. Sub-basin scale dust source geomorphology detected using MODIS. Geophys. Res. Lett. 25, L15404.
Bullard, J.E., Harrison, S.P., Baddock, M.C., Drake, N., Gill, T.E., McTainsh, G., Sun, Y., 2011. Preferential dust sources: a geomorphological classification designed for use in global dust-cycle models. J. Geophys. Res. 116, F04034.
Cahill, T.A., Gill, T.E., Reid, J.S., Gearhart, E.A., Gillette, D.A., 1996. Saltating particles, playa crusts and dust aerosols at Owens (dry) Lake, California. Earth Surf. Process. Landforms 21, 621–639.
Castiglia, P.J., Fawcett, P.J., 2006. Large holocene lakes and climate change in the Chihuahuan Desert. Geology 34, 113–116.
Cooley, S.W., Smith, L.C., Stepan, L., Mascaro, J., 2017. Tracking dynamic northern surface water changes with high-frequency Planet CubeSat imagery. Rem. Sens. 9, 1306.
Cui, M., Lu, H., Wiggs, G.F., Etyemezian, V., Sweeney, M.R., Xu, Z., 2019. Quantifying the effect of geomorphology on aeolian dust emission potential in northern China. Earth Surf. Process. Landforms 44, 2872–2884.
d'Angelo, P., Máttyus, G., Reinartz, P., 2016. Skybox image and video product evaluation. Int. J. Image Data Fusion 7, 3–18.
da Silva Curiel, A., Boland, L., Cooksley, J., Bekhti, M., Stephens, P., Sun, W., Sweeting, M., 2005. First results from the disaster monitoring constellation (DMC). Acta Astronaut. 56, 261–271.
Dominguez Acosta, M., 2009. The Pluvial Lake Palomas-Samalyuca Dunes System. Ph.D. Dissertation (Geological Sciences). University of Texas at El Paso.
Eckardt, F.D., Kuring, N., 2005. SeaWiFS identifies dust sources in the Namib Desert. Int. J. Rem. Sens. 26, 4159–4167.
Field, J.P., Breshears, D.D., Whicker, J.J., 2009. Toward a more holistic perspective of soil erosion: why aeolian research needs to explicitly consider fluvial processes and interactions. Aeolian Res. 1, 9–17.
Floyd, K.W., Gill, T.E., 2011. The association of land cover with aeolian sediment production at Jornada Basin, New Mexico, USA. Aeolian Res. 3, 55–66.
Gasch, P., Rieger, D., Walter, C., Khain, P., Levi, Y., Knippertz, P., Vogel, B., 2017. Revealing the meteorological drivers of the September 2015 severe dust event in the Eastern Mediterranean. Atmos. Chem. Phys. 17, 13573–13604.
Gill, T.E., 1996. Eolian sediments generated by anthropogenic disturbance of playas: human impacts on the geomorphic system and geomorphic impacts on the human system. Geomorphology 17, 207–228.
Gillette, D.A., 1999. A qualitative geophysical explanation for hot spot dust emitting source regions. Contrib. Atmos. Phys. 72 (1), 67–78.
Ginoux, P., Garbuzov, D., Hsu, N.C., 2010. Identification of anthropogenic and natural dust sources using Moderate Resolution Imaging Spectroradiometer (MODIS) Deep Blue level 2 data. J. Geophys. Res. 115, D05204.
Ginoux, P., Prospero, J.M., Gill, T.E., Hsu, N.C., Zhao, M., 2012. Global-scale attribution of anthropogenic and natural dust sources and their emission rates based on MODIS Deep Blue aerosol products. Rev. Geophys. 50, RG3005.
Hahnenberger, M., Nicoll, K., 2014. Geomorphic and land cover identification of dust sources in the eastern Great Basin of Utah, USA. Geomorphology 204, 657–672.
Haustein, K., Washington, R., King, J., Wiggs, G., Thomas, D.S.G., Eckardt, F.D., Bryant, R.G., Menut, L., 2015. Testing the performance of state-of-the-art dust emission schemes using DO4Models field data. Geosci. Model Dev. (GMD) 8, 341–362.
Heinold, B., Tegen, I., Schepanski, K., Banks, J.R., 2016. New developments in the representation of Saharan dust sources in the aerosol-climate model ECHAM6-HAM2. Geosci. Model Dev. (GMD) 9, 765–777.
Hennen, M., White, K., Shahgedanova, M., 2019. An assessment of SEVIRI imagery at various temporal resolutions and the effect on accurate dust emission mapping. Rem. Sens. 11, 918.
Hsu, N.C., Jeon, M.-J., Bettenhausen, C., Sayer, A.M., Hansell, R., Seftor, C.S., Huang, J., Tsay, S.-C., 2013. Enhanced Deep Blue aerosol retrieval algorithm: the second generation. J. Geophys. Res. 118, 9296–9315.
INEGI (Instituto Nacional de Estadística, Geografía y Informática), México, 2001. Sistema de Topoformas. Available online at: http://en.www.inegi.org.mx/temas/fisiografia/default.html#Downloads. Accessed 25th May 2020.
Kandakji, T., Gill, T.E., Lee, J.A., 2020. Identifying and characterizing dust point sources in the southwestern United States using remote sensing and GIS. Geomorphology 353, 107019.
Kaufman, Y.J., Tanré, D., Boucher, O., 2002. A satellite view of aerosols in the climate system. Nature 419, 215–223.
King, J., Etyemezian, V., Sweeney, M., Buck, B.J., Nikolich, G., 2011. Dust emission variability at the salton sea, California, USA. Aeolian Res. 3, 67–79.
Klose, M., Gill, T.E., Etyemezian, V., Nikolich, G., Zadeh, Z.G., Webb, N.P., Van Pelt, R.S., 2019. Dust emission from crusted surfaces: insights from field measurements and modelling. Aeolian Res. 40, 1–14.
Kocurek, G., Lancaster, N., 1999. Aeolian system sediment state: theory and Mojave Desert Kelso dune field example. Sedimentology 46, 505–515.
Kok, J.F., Mahowald, N.M., Albani, S., Fratini, G., Gillies, J.A., Ishizuka, M., Leys, J.F., Mikami, M., Park, M.S., Park, S.U., Van Pelt, R.S., 2014. An improved dust emission model with insights into the global dust cycle's climate sensitivity. Atmos. Chem. Phys. 14, 13023–13041.
Kondragunta, S., Zhang, H., Ciren, P., Laszlo, I., Tong, D., 2018. Tracking dust storms using the latest satellite technology: the rapid refresh GOES-16 advanced baseline imager. May 2018 Equip. Manag.: Mag. Environ. Manag. 25–30.
Kopacz, J.R., Herschitz, R., Roney, J., 2020. Small satellites: an overview and assessment. Acta Astronaut. 170, 93–105.
Lancaster, N., Baas, A., 1998. Influence of vegetation cover on sand transport by wind: field studies at Owens Lake, California. Earth Surf. Process. Landforms 23, 69–82.
Lee, J.A., Gill, T.E., Mulligan, K.R., Dominguez Acosta, M., Perez, A.E., 2009. Land use/land cover and point sources of the 15 December 2003 dust storm in southwestern North America. Geomorphology 105, 18–27.
Lee, J.A., Baddock, M.C., Mbuh, M.J., Gill, T.E., 2012. Geomorphic and land cover characteristics of aeolian dust sources in west Texas and eastern New Mexico, USA. Aeolian Res. 3, 459–466.
Li, J., Roy, D.P., 2017. A global analysis of Sentinel-2A, Sentinel-2B and Landsat-8 data revisit intervals and implications for terrestrial monitoring. Rem. Sens. 9, 902.
Li, J., Kandakji, T., Lee, J.A., Tatarko, J., Blackwell III, J., Gill, T.E., Collins, J.D., 2018. Blowing dust and highway safety in the southwestern United States: characteristics of dust emission "hotspots" and management implications. Sci. Total Environ. 621, 1023–1032.
Liu, S., Hodgson, M.E., 2016. Satellite image collection modeling for large area hazard emergency response. ISPRS J. Photogrammetry Remote Sens. 118, 13–21.
Mahowald, N.M., Bryant, R.G., del Corral, J., Steinberger, L., 2003. Ephemeral lakes and desert dust sources. Geophys. Res. Lett. 30, 1074.
Mahowald, N.M., Kloster, S., Engelstaedter, S., Moore, J.K., Mukhopadhyay, S., McConnell, J.R., Albani, S., Doney, S.C., Bhattacharya, A., Curran, M.A.J., Flanner, M.G., Hoffman, F.M., Lawrence, D.M., Lindsay, K., Mayewski, P.A., Neff, J., Rothenberg, D., Thomas, E., Thornton, P.E., Zender, C.S., 2010. Observed 20th century desert dust variability: impact on climate and biogeochemistry. Atmos. Chem. Phys. 10, 10875–10893.
Miller, S.D., 2003. A consolidated technique for enhancing desert dust storms with MODIS. Geophys. Res. Lett. 30, 2071.
Miller, M.E., Bowker, M.A., Reynolds, R.L., Goldstein, H.L., 2012. Post-fire land treatments and wind erosion - lessons from the milford flat fire, UT, USA. Aeolian Res. 7, 29–44.
Muhs, D.R., Prospero, J.M., Baddock, M.C., Gill, T.E., 2014. Identifying sources of aeolian mineral dust: present and past. In: Stuut, J.-B., Knippertz, P. (Eds.), Mineral Dust – a Key Player in the Earth System. Springer, Berlin, pp. 51–74.
Murray, J.E., Brindley, H.E., Bryant, R.G., Russell, J.E., Jenkins, K.F., Washington, R., 2016. Enhancing weak transient signals in SEVIRI false color imagery: application to dust source detection in southern Africa. J. Geophys. Res. 121, 10199–10219.
Novlan, D.J., Hardiman, M., Gill, T.E., 2007. A Synoptic Climatology of Blowing Dust Events in El Paso, Texas from 1932–2005. Preprints, 16th Conf. on Applied Climatology. Amer. Meteorol. Soc.. J3.12.
Nicoll, K., Hahnenberger, M., Goldstein, H.L., 2020. 'Dust in the wind' from source-to-sink: analysis of the 14-15 April 2015 storm in Utah. Aeolian Res. 46, 100532.
O'Loingsigh, T., McTainsh, G.H., Tapper, N.J., Shinkfield, P., 2010. Lost in code: a critical analysis of using meteorological data for wind erosion monitoring. Aeolian Res. 2, 49–57.
O'Loingsigh, T., Mitchell, R.M., Campbell, S.K., Drake, N.A., McTainsh, G.H., Tapper, N. J., Dunkerley, D.L., 2015. Correction of dust event frequency from MODIS Quick-Look imagery using in-situ aerosol measurements over the Lake Eyre Basin, Australia. Rem. Sens. Environ. 169, 222–231.
Parajuli, S.P., Zender, C.S., 2017. Connecting geomorphology to dust emission through high-resolution mapping of global land cover and sediment supply. Aeolian Res. 27, 47–65.
Parajuli, S.P., Yang, Z.L., Kocurek, G., 2014. Mapping erodibility in dust source regions based on geomorphology, meteorology, and remote sensing. J. Geophys. Res. 119, 1977–1994.
Park, S.H., Jung, H.S., Lee, M.J., Lee, W.J., Choi, M.J., 2019. Oil spill detection from PlanetScope satellite image: application to oil spill accident near ras Al zour area, Kuwait in august 2017. J. Coastal Res. Suppl. 90, 251–260.
Planet Labs, 2020. Imagery and Archive Details available at: https://www.planet.com/products/planet-imagery/. Accessed 1st June 2020.
Plekhov, D., Levine, E.I., 2018. Assessing the effects of severe weather events through remote sensing on Samothrace, Greece: applications for management of cultural resources. J. Arch. Sci. Rep. 21, 810–820.
Prospero, J.M., Ginoux, P., Torres, O., Nicholson, S.E., Gill, T.E., 2002. Environmental characterization of global sources of atmospheric soil dust identified with the Nimbus 7 Total Ozone Mapping Spectrometer (TOMS) absorbing aerosol product. Rev. Geophys. 40, 1002.
Reynolds, R.L., Yount, J.C., Reheis, M., Goldstein, H., Chavez Jr., P., Fulton, R., Whitney, J., Fuller, C., Forester, R.M., 2007. Dust emission from wet and dry playas in the Mojave Desert, USA. Earth Surf. Process. Landforms 32, 1811–1827.
Richter, D., Gill, T., 2018. Challenges and opportunities in atmospheric dust emission, chemistry, and transport. Bull. Am. Meteorol. Soc. 99, ES115–ES118.
Rivas Jr., J.A., Schröder, T., Gill, T.E., Wallace, R.L., Walsh, E.J., 2019. Anemochory of diapausing stages of microinvertebrates in North American drylands. Freshw. Biol. 64, 1303–1314.
Rivera Rivera, N.I., Gill, T.E., Gebhart, K.A., Hand, J.L., Bleiweiss, M.P., Fitzgerald, R.M., 2009. Wind modeling of Chihuahuan Desert dust events. Atmos. Environ. 43, 347–354.
Rivera Rivera, N.I., Gill, T.E., Bleiweiss, M.P., Hand, J.L., 2010. Source characteristics of hazardous Chihuahuan Desert dust outbreaks. Atmos. Environ. 44, 2457–2468.

Rosen, M.R., 1994. The importance of groundwater in playas: a review of playa classifications and the sedimentology and hydrology of playas. Geol. Soc. Am. Spec. Pap. 289, 1–18.
Schepanksi, K., Tegen, I., Laurent, B., Heinold, B., Macke, A., 2007. A new Saharan dust source activation frequency map derived from MSG-SEVIRI IR-channels. Geophys. Res. Lett. 34, L18803.
Schepanski, K., Tegen, I., Todd, M.C., Heinold, B., Bönisch, G., Laurent, B., Macke, A., 2009. Meteorological processes forcing Saharan dust emission inferred from MSG-SEVIRI observations of subdaily dust source activation and numerical models. J. Geophys. Res. 114, D10201.
Schepanski, K., Tegen, I., Macke, A., 2012. Comparison of satellite based observations of Saharan dust source areas. Remote Sens. Environ. 123, 90–97.
Schmetz, J., Pili, P., Tjemkes, S., Just, D., Kerkmann, J., Rota, S., Ratier, A., 2002. An introduction to Meteosat second generation (MSG). Bull. Am. Meteorol. Soc. 83, 977–992.
Shao, Y., Wyrwoll, K.H., Chappell, A., Huang, J., Lin, Z., McTainsh, G.H., Mikami, M., Tanaka, T.Y., Wang, X., Yoon, S., 2011. Dust cycle: an emerging core theme in Earth system science. Aeolian Res. 2, 181–204.
Sinclair, S.N., LeGrand, S.L., 2019. Reproducibility assessment and uncertainty quantification in subjective dust source mapping. Aeolian Res. 40, 42–52.
She, L., Xue, Y., Yang, X., Guang, J., Li, Y., Che, Y., Fan, C., Xie, Y., 2018. Dust detection and intensity estimation using Himawari-8/AHI observation. Rem. Sens. 10, 490.
Sowden, M., Mueller, U., Blake, D., 2018. Review of surface particulate monitoring of dust events using geostationary satellite remote sensing. Atmos. Environ. 183, 154–164.
Sweeney, M.R., McDonald, E.V., Etyemezian, V., 2011. Quantifying dust emissions from desert landforms, eastern Mojave Desert, USA. Geomorphology 135, 21–34.
Thomas, D.S.G., Wiggs, G.F.S., 2008. Aeolian system responses to global change: challenges of scale, process and temporal integration. Earth Surf. Process. Landforms 33, 1396–1418.
Thompson, D., Braverman, A., Brodrick, P.G., Candela, A., Carmon, N., Clark, R.N., Connely, D., Green, R.O., Kokaly, R.F., Li, L., Mahowald, N., Miller, R.L., Oking, G.S., Painter, T.H., Swayze, G.A., Turmon, M., Susilouto, J., Wettergreen, D.S., 2020. Quantifying uncertainty for remote spectroscopy of surface composition. Remote Sens. Environ. 247, 111898.
Urban, F.E., Goldstein, H.L., Fulton, R., Reynolds, R.L., 2018. Unseen dust emission and global dust abundance: documenting dust emission from the Mojave Desert (USA) by daily remote camera imagery and wind-erosion measurements. J. Geophys. Res. 123, 8735–8753.
Vickery, K.J., Eckardt, F.D., Bryant, R.G., 2013. A sub-basin scale dust plume source frequency inventory for southern Africa, 2005-2008. Geophys. Res. Lett. 40, 5274–5279.
von Holdt, J.R., Eckardt, F.D., Wiggs, G.F.S., 2017. Landsat identifies aeolian dust emission dynamics at the landform scale. Remote Sens. Environ. 198, 229–243.
von Holdt, J.R.C., Eckardt, F.D., Baddock, M.C., Wiggs, G.F.S., 2019. Assessing landscape dust emission potential using combined ground-based measurements and remote sensing data. J. Geophys. Res. 124, 1080–1098.
Villela, T., Costa, C.A., Brandão, A.M., Bueno, F.T., Leonardi, R., 2019. Towards the thousandth CubeSat: a statistical overview. Int. J. Aero. Eng., 063145, 2019.
Walker, A.L., Liu, M., Miller, S.D., Richardson, K.A., Westphal, D.L., 2009. Development of a dust source database for mesoscale forecasting in Southwest Asia. J. Geophys. Res. 114, D18207.
Washington, R., Todd, M., Middleton, N.J., Goudie, A.S., 2003. Dust storm source areas determined by the Total Ozone Monitoring Spectrometer and surface observations. Ann. Assoc. Am. Geogr. 93, 297–313.
Webb, N.P., Strong, C.L., 2011. Soil erodibility dynamics and its representation for wind erosion and dust emission models. Aeolian Res. 3, 165–179.
Webb, N.P., Herrick, J.E., Van Zee, J.W., Courtright, E.M., Hugenholtz, C.H., Zobeck, T. M., Okin, G.S., Clingan, S.D., Cooper, B.F., Billings, B.J., Boyd, R., Duniway, M.C., Derner, J.D., Fox, F.A., Havstad, K.M., Heilman, P., Ludwig, N.A., Metz, L.J., Nearing, M.A., Norfleet, M.L., Pierson, F.B., Sanderson, M.A., Sharratt, B.S., Steiner, J.L., Tatarko, J., Tedela, N.H., Toledo, D., Unnasch, R.S., Van Pelt, R.S., Wagner, L., 2016. The National Wind Erosion Research Network: building a standardized long-term data resource for aeolian research, modeling and land management. Aeolian Res. 22, 23–36.
Webb, N.P., Chappell, A., Edwards, B.L., McCord, S.E., Van Zee, J.W., Cooper, B.F., Courtright, E.M., Duniway, M.C., Sharratt, B., Tedela, N., Toledo, D., 2019. Reducing sampling uncertainty in aeolian research to improve change detection. J. Geophys. Res. 124, 1366–1377.
Wicaksono, P., Lazuardi, W., 2018. Assessment of PlanetScope images for benthic habitat and seagrass species mapping in a complex optically shallow water environment. Int. J. Rem. Sens. 39, 5739–5765.
Yue, H., He, C., Zhao, Y., Ma, Q., Zhang, Q., 2017. The brightness temperature adjusted dust index: an improved approach to detect dust storms using MODIS imagery. Int. J. Appl. Earth Obs. Geoinf. 57, 166–176.
Zender, C.S., Newman, D.J., Torres, O., 2003. Spatial heterogeneity in aeolian erodibility: uniform, topographic, geomorphic and hydrologic hypotheses. J. Geophys. Res. 108, 4543.
Zhang, B., Tsunekawa, A., Tsubo, M., 2008. Contributions of sandy lands and stony deserts to long-distance dust emission in China and Mongolia during 2000-2006. Global Planet. Change 60, 487–504.